Regulation of connexin43 gap junctional communication by phosphatidylinositol 4,5-bisphosphate

Leonie van Zeijl,[1] Bas Ponsioen,[1,2] Ben N.G. Giepmans,[1] Aafke Ariaens,[1] Friso R. Postma,[1] Péter Várnai,[3] Tamas Balla,[3] Nullin Divecha,[1] Kees Jalink,[2] and Wouter H. Moolenaar[1]

[1]Division of Cellular Biochemistry, Centre for Biomedical Genetics, and [2]Division of Cell Biology, The Netherlands Cancer Institute, 1066 CX Amsterdam, Netherlands
[3]Endocrinology and Reproduction Research Branch, National Institute of Child Health and Human Development, National Institutes of Health, Bethesda, MD 20892

Cell–cell communication through connexin43 (Cx43)-based gap junction channels is rapidly inhibited upon activation of various G protein–coupled receptors; however, the mechanism is unknown. We show that Cx43-based cell–cell communication is inhibited by depletion of phosphatidylinositol 4,5-bisphosphate (PtdIns[4,5]P_2) from the plasma membrane. Knockdown of phospholipase Cβ3 (PLCβ3) inhibits PtdIns(4,5)P_2 hydrolysis and keeps Cx43 channels open after receptor activation. Using a translocatable 5-phosphatase, we show that PtdIns(4,5)P_2 depletion is sufficient to close Cx43 channels. When PtdIns(4,5)P_2 is overproduced by PtdIns(4)P 5-kinase, Cx43 channel closure is impaired. We find that the Cx43 binding partner zona occludens 1 (ZO-1) interacts with PLCβ3 via its third PDZ domain. ZO-1 is essential for PtdIns(4,5)P_2-hydrolyzing receptors to inhibit cell–cell communication, but not for receptor–PLC coupling. Our results show that PtdIns(4,5)P_2 is a key regulator of Cx43 channel function, with no role for other second messengers, and suggest that ZO-1 assembles PLCβ3 and Cx43 into a signaling complex to allow regulation of cell–cell communication by localized changes in PtdIns(4,5)P_2.

Introduction

Communication between adjacent cells through gap junctions occurs in nearly every tissue and is fundamental to coordinated cell behavior. Gap junctions are composed of connexins, consisting of an intracellular N terminus, four transmembrane domains, and a cytosolic C-terminal tail. Six connexins oligomerize into a pore-forming connexon, and alignment of two connexons in apposing cell membranes forms a gap junction channel.

These channels allow direct cell-to-cell diffusion of ions and small molecules (<1–2 kD), including nutrients, metabolites, second messengers, and peptides, without transit through the extracellular space (Goodenough et al., 1996; Harris, 2001; Saez et al., 2003). Gap junctions play important roles in normal tissue function and organ development (Reaume et al., 1995; Sohl and Willecke, 2004; Wei et al., 2004) and have been implicated in a great diversity of biological processes, notably, electrical synchronization of excitable cells, energy metabolism, growth control, wound repair, tumor cell invasion, and antigen cross-presentation (Kwak et al., 2001; Qiu et al., 2003; Mesnil et al., 2005; Oliveira et al., 2005; Neijssen et al., 2005; Bernstein and Morley, 2006; Mori et al., 2006). The importance of gap junctions is highlighted by the discovery that mutations in connexins underlie a variety of genetic diseases, including peripheral neuropathy, skin disorders, and deafness (Gerido and White, 2004; Wei et al., 2004).

Connexin43 (Cx43) is the most abundant and best-studied mammalian connexin. Cx43-based gap junctional communication is of a particular interest because it is regulated by both physiological and pathophysiological stimuli. In particular, Cx43-based

cell–cell coupling is rapidly disrupted after stimulation of certain G protein–coupled receptors (GPCRs), such as those for endothelin, thrombin, nucleotides, and bioactive lipids (Hill et al., 1994; Venance et al., 1995; Postma et al., 1998; Spinella et al., 2003; Meme et al., 2004; Blomstrand et al., 2004; Rouach et al., 2006). Disruption is transient, as communication is restored after ~20–60 min, depending on the GPCR involved (Postma et al., 1998). GPCR-mediated inhibition of intercellular communication will have broad consequences for long-range signaling in cells and tissues where Cx43 is vital, such as dermal fibroblasts, glial cells, and heart. However, the link between receptor stimulation and Cx43 channel closure has remained elusive to date. Numerous studies on the "gating" of Cx43 channels have focused on a possible role for phosphorylation of Cx43 by various protein kinases, in particular, PKC, MAP kinase, and c-Src, but the results remain ambiguous (Lampe and Lau, 2004; Warn-Cramer and Lau, 2004; Laird, 2005). One of the difficulties with unraveling the regulation of Cx43 channel function is that Cx43 functions in a multiprotein complex that is currently ill understood (Giepmans, 2004). One established component of this assembly is the scaffold protein zona occludens 1 (ZO-1), which binds directly to the C terminus of Cx43 via its second PDZ domain (Giepmans and Moolenaar, 1998; Toyofuku et al., 1998). ZO-1 has been suggested to participate in the assembly and proper distribution of gap junctions, but its precise role in the Cx43 complex remains unclear (Hunter et al., 2005; Laing et al., 2005).

In the present study, we sought to identify the signaling pathway that leads to inhibition of Cx43 gap junctional communication in fibroblasts. Using a variety of experimental approaches, we show that the levels of phosphatidylinositol 4,5-bisphosphate (PtdIns[4,5]P$_2$) at the plasma membrane dictate the inhibition (and restoration) of Cx43 gap junctional communication in response to GPCR stimulation, with no role for PtdIns(4,5)P$_2$-derived second messengers. We further show that ZO-1, via its third PDZ domain, interacts with phospholipase Cβ3 (PLCβ3) and is essential for G$_q$/PLC-coupled receptors to abrogate Cx43-based cell–cell communication. Our results suggest a model in which ZO-1 serves to organize Cx43 and PLCβ3 into a complex to allow exquisite regulation of Cx43 channel function by localized changes in PtdIns(4,5)P$_2$.

Results

Regulation of Cx43 gap junctional communication by the Gα$_q$/PLCβ–PtdIns(4,5)P$_2$ hydrolysis pathway

Rat-1 fibroblasts are ideally suited for studying Cx43 channel function because they express Cx43 as the only functional connexin (Postma et al., 1998; Ponsioen et al., 2007). Stable knockdown of Cx43 expression (using pSuper short hairpin RNA [shRNA]) resulted in a complete loss of intercellular communication, consistent with Cx43 being the only functional gap junction protein in Rat-1 cells (Fig. 1 A). Fig. 1 B shows that the Cx43 binding partner ZO-1 retains its submembranous localization in Cx43-knockdown cells.

To assess which G proteins mediate inhibition of gap junctional communication, we introduced active versions of
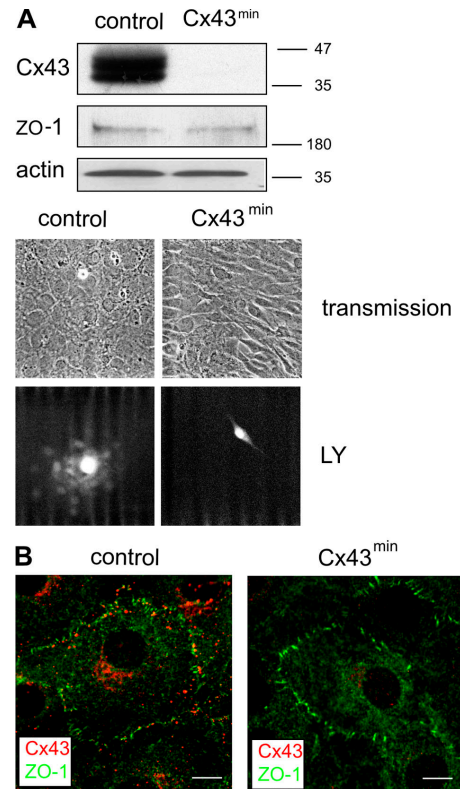
Figure 1. **Cx43 is the only functional connexin in Rat-1 cells.** (A) Rat-1 cells were transduced with Cx43 shRNA (Cx43^{min}) or with a nonfunctional shRNA (control). (top) Immunoblot showing that stable expression of Cx43 shRNA leads to the disappearance of Cx43 (Cx43^{min} cells) while leaving ZO-1 expression unaltered. Actin served as loading control. (bottom) Wide-field images of control and Cx43^{min} Rat-1 cells. Cx43^{min} cells lack cell–cell communication, as determined by LY diffusion. (B) Confocal images of control and Cx43^{min} cells immunostained for Cx43 (red) and ZO-1 (green). Bars, 5 μm.

Gα$_q$, Gα$_i$, Gα$_{12}$, and Gα$_{13}$ subunits into Rat-1 cells and examined their impact on cell–cell coupling. Expression of active Gα$_q$ resulted in complete inhibition of intercellular communication, whereas active Gα$_i$, Gα$_{12}$, and Gα$_{13}$ left cell–cell coupling unaltered, as indicated by Lucifer yellow (LY) diffusion and electrophysiological assays (Fig. 2 A). Disruption of gap junctional communication induced by active Gα$_q$ was persistent, as opposed to the transient inhibition observed after GPCR stimulation (Postma et al., 1998). Similarly, treatment of Rat-1 cells with *Pasteurella multocida* toxin, a direct activator of Gα$_q$ (Orth et al., 2005), caused persistent abrogation of cell–cell coupling (Fig. 2 B). Gα$_q$ couples to PLCβ to trigger PtdIns(4,5)P$_2$ hydrolysis, leading to production of the second messengers inositol-1,4,5-trisphosphate (IP$_3$) and DAG (Rhee, 2001). We monitored PtdIns(4,5)P$_2$ in living cells by using a GFP fusion protein of the pleckstrin homology (PH) domain of PLCδ1 (GFP-PH) as a probe (Stauffer et al., 1998; Varnai and Balla, 1998; van der Wal et al., 2001). In control cells, the PtdIns(4,5)P$_2$ probe was concentrated at the plasma membrane. In cells expressing active Gα$_q$, however, the probe was spread diffusely throughout the cytosol, indicative of PtdIns(4,5)P$_2$ depletion from the plasma membrane (Fig. 2 C). Although these results are consistent with Gα$_q$ mediating agonist-induced inhibition of intercellular communication, they should be interpreted with caution because
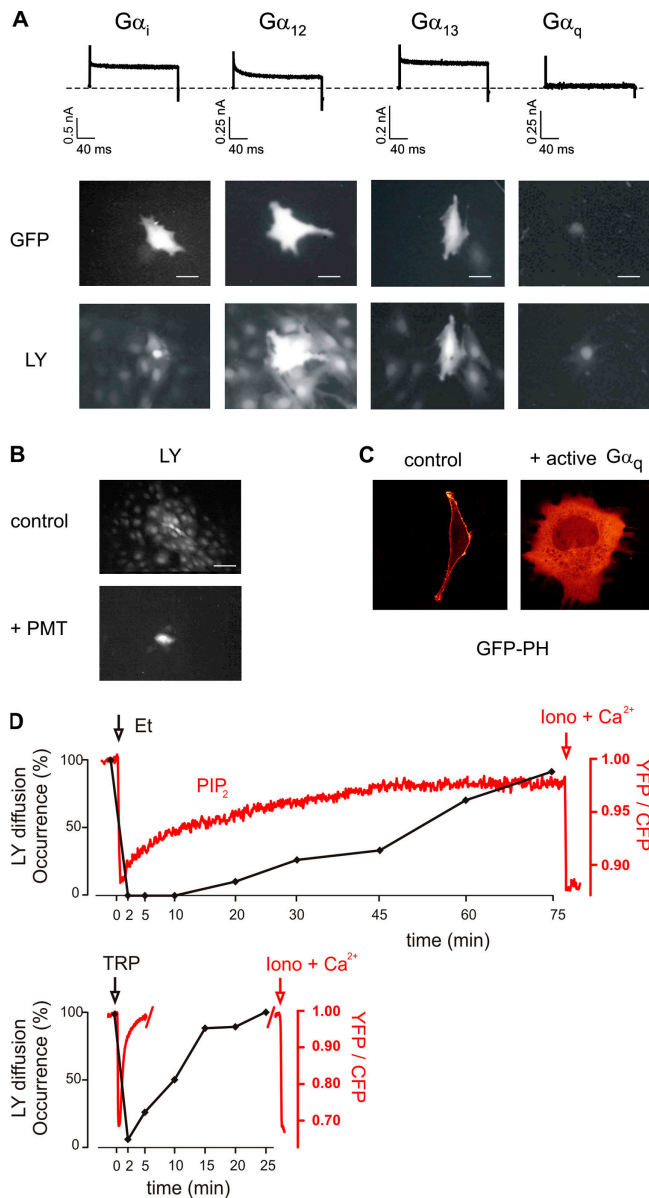
Figure 2. **Activated Gα$_q$ disrupts Cx43-based gap junctional communication: correlation with PtdIns(4,5)P$_2$ depletion.** (A) Intercellular communication in Rat-1 cells transfected with various activated (GTPase-deficient) Gα subunits. (top) Electrical cell–cell coupling measured by a single patch-clamp electrode (Postma et al., 1998). Whole-cell current responses to 10-mV voltage pulses (duration, 100 ms; holding potential, −70 mV) were recorded from confluent Rat-1 cells. Note the dramatic increase in cellular input resistance (i.e., a decrease in conductance) by activated Gα$_q$ but not other Gα subunits. (middle and bottom) Rat-1 cells cotransfected with active Gα subunits and GFP (10:1 ratio). GFP-positive cells were microinjected with LY, and dye diffusion from the microinjected cells was monitored. Wide-field pictures of GFP and LY diffusion as indicated. Bars, 10 μm. (B) Disruption of gap junctional communication by 1 μg/ml *P. multocida* toxin (PMT; 3-h preincubation), an activator of Gα$_q$, as measured by LY diffusion. Bar, 20 μm. (C) Depletion of PtdIns(4,5)P$_2$ from the plasma membrane by activated Gα$_q$. HEK293T cells were transfected with the PtdIns(4,5)P$_2$ sensor GFP-PH, alone or together with active Gα$_q$ (1:10 ratio). GFP-PH localizes to the plasma membrane, where it binds PtdIns(4,5)P$_2$ (left). Coexpression with activated Gα$_q$ causes GFP-PH to relocalize to the cytosol (right). (D) Monitoring PtdIns(4,5)P$_2$ levels (PIP$_2$; red trace) and intercellular communication (black; $n \geq 20$ per time point) in Rat-1 cells after addition of 50 nM endothelin (top) or 50 μM TRP (bottom). Data points show the percentage of injected cells that spread LY to their neighbors. Temporal changes in plasma membrane–bound PtdIns(4,5)P$_2$ were measured by changes in FRET between CFP-PH and YFP-PH. Ionomycin, which evokes an immediate

constitutive depletion of PtdIns(4,5)P$_2$ from the plasma membrane promotes apoptosis (Kranenburg et al., 1999; Halstead et al., 2006).

To monitor the kinetics of PtdIns(4,5)P$_2$ hydrolysis and resynthesis with high temporal resolution, we made use of the fluorescence resonance energy transfer (FRET) between the PH domains of PLCδ1 fused to CFP and YFP, respectively (van der Wal et al., 2001). When bound to plasma membrane PtdIns(4,5)P$_2$, CFP-PH and YFP-PH are in close proximity and show FRET. After PtdIns(4,5)P$_2$ breakdown, the probes dilute out into the cytosol, and FRET ceases. The prototypic G$_q$-coupled receptor agonist endothelin, acting through endogenous endothelin A receptors, induced an acute and substantial decrease in PtdIns(4,5)P$_2$, reaching a maximum after 30–60 s; thereafter, PtdIns(4,5)P$_2$ slowly recovered to near basal levels over a period lasting as long as 45–60 min (Fig. 2 D, top, red trace). Sustained PtdIns(4,5)P$_2$ hydrolysis by endothelin A receptors has been reported previously (Cramer et al., 1997) and may be explained by the fact that activated endothelin A receptors follow a recycling pathway back to the cell surface rather than the lysosomal degradation route (Bremnes et al., 2000). The kinetics of endothelin-induced inhibition and recovery of cell–cell communication followed those of PtdIns(4,5)P$_2$ hydrolysis and resynthesis, respectively, with communication being restored after ∼75 min (Fig. 2 D, top, black trace).

More transient PtdIns(4,5)P$_2$ depletion and recovery kinetics were observed with a thrombin receptor (PAR-1 [protease-activated receptor 1]) activating peptide (TRP), which correlated with a more short-lived inhibition of gap junctional communication (Fig. 2 D, bottom). Furthermore, a desensitization-defective mutant NK2 receptor (for neurokinin A) that mediates prolonged PtdIns(4,5)P$_2$ hydrolysis (Alblas et al., 1996) inhibits gap junctional communication for prolonged periods of time when compared with the wild-type NK2 receptor (Postma et al., 1998). Although these results reveal a close correlation between the duration of PtdIns(4,5)P$_2$ depletion and that of communication shutoff, we note that the restoration of cell–cell communication consistently lagged behind the recovery of PtdIns(4,5)P$_2$ levels. Nevertheless, our findings strongly suggest that the G$_q$/PLCβ-mediated hydrolysis and subsequent resynthesis of PtdIns(4,5)P$_2$ dictate the inhibition and restoration of Cx43 gap junctional communication, respectively.

Knockdown of PLCβ3 prevents cell–cell uncoupling

The Gα$_q$-activated PLCβ enzymes comprise four members (β1–4; Rhee, 2001). PLCβ1 and -β3 are ubiquitously expressed, whereas PLCβ2 and -β4 expression is restricted to hematopoietic cells and neurons, respectively. Rat-1 cells express PLCβ3 but no detectable PLCβ1 (Fig. 3 A and not depicted). We stably suppressed PLCβ3 expression using the pSuper shRNA expression vector (Brummelkamp et al., 2002). Four different target sequences were selected to correct for clonal variation and off-target effects. Immunoblot analysis shows a marked reduction

and complete depletion of PtdIns(4,5)P$_2$ from the plasma membrane when applied at high doses (5 μM), together with 5 mM Ca^{2+} (van der Wal et al., 2001) was used for calibration.
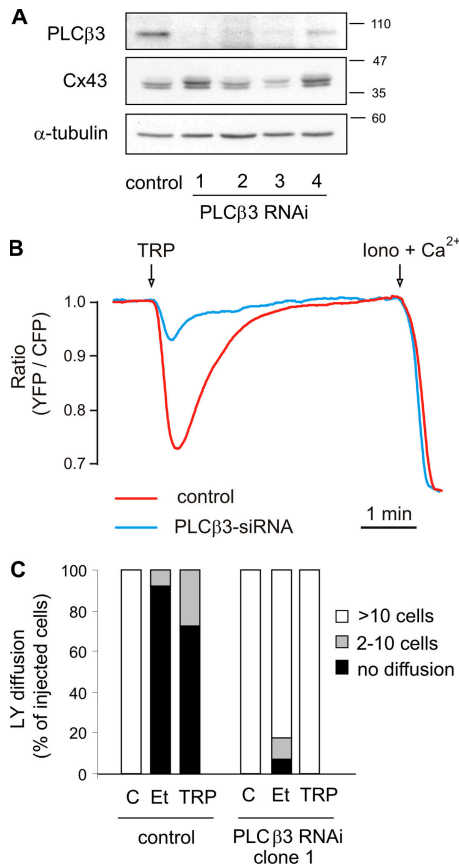
Figure 3. Targeted knockdown of PLCβ3 prevents receptor-mediated PtdIns(4,5)P₂ hydrolysis and inhibition of junctional communication. (A) PLCβ3 knockdown in Rat-1 cells as detected by immunoblotting. Expression of PLCβ3 in Rat-1 cells expressing a nonfunctional shRNA (control) and in four subclones (1–4) stably expressing different PLCβ3 shRNA constructs. Total cell lysates were immunoblotted for PLCβ3, Cx43, and α-tubulin as indicated. (B) Temporal changes in plasma membrane PtdIns(4,5)P₂ levels after thrombin receptor stimulation of normal (red trace) and PLCβ3-deficient Rat-1 cells (blue trace). TRP was used at 50 μM, and Ionomycin was used at 5 μM. $n = 5$. (C) Bar graphs showing the percentage of communicating cells in control and PLCβ3-knockdown cells (clone 1) treated with either 50 nM endothelin (Et) or 50 μM TRP, as indicated ($n \geq 25$ for each dataset). LY injections were done at 2 min after addition of agonist.

in PLCβ3 expression in different clones (Fig. 3 A). When comparing PtdIns(4,5)P₂ dynamics in PLCβ3-knockdown versus control cells, agonist-induced PtdIns(4,5)P₂ breakdown was strongly reduced in the PLCβ3-deficient cells (Fig. 3 B). PLCβ3-knockdown cells showed normal basal cell–cell communication but failed to shut off cell–cell communication after GPCR stimulation (Fig. 3 C). These results indicate that PLCβ3 is a key player in the control of intercellular communication, supporting the view that GPCRs inhibit gap junctional communication through the G$_q$/PLCβ3–PtdIns(4,5)P₂ hydrolysis pathway.

PLC-mediated PtdIns(4,5)P₂ hydrolysis generates the second messengers IP₃ and DAG, leading to Ca²⁺ mobilization and PKC activation, respectively. Previous pharmacological studies have already suggested that neither Ca²⁺ nor PKC have a critical role in GPCR-mediated inhibition of cell–cell coupling (Postma et al., 1998), a notion supported by additional experiments using "caged" IP₃, the cell-permeable Ca²⁺ chelator BAPTA-AM (1,2-bis[2-aminophenoxy]ethane-N,N,N,N-tetra-

acetic acid), and a PKC-activating bacterial PLC (van Dijk et al., 1997; Table S1, available at http://www.jcb.org/cgi/content/full/jcb.200610144/DC1). Whether PtdIns(4,5)P₂-derived second messengers are dispensable for Cx43 channel closure upon GPCR activation remains debatable, however, as the supporting pharmacological evidence is indirect.

Conversion of PtdIns(4,5)P₂ into PtdIns(4)P by phosphoinositide 5-phosphatase is sufficient to inhibit cell–cell communication

To examine whether the depletion of PtdIns(4,5)P₂ suffices to inhibit Cx43 gap junctional communication, we used a newly developed method to rapidly deplete PtdIns(4,5)P₂ without activating PLC. In this approach, PtdIns(4,5)P₂ at the plasma membrane is converted into PtdIns(4)P and free phosphate by rapamycin-inducible membrane targeting of the human type IV phosphoinositide 5-phoshatase (5-ptase; Suh et al., 2006; Varnai et al., 2006). The method is based on the rapamycin-induced heterodimerization of FRB (fragment of mammalian target of rapamycin that binds FKB12) and FKB12 (FK506 binding protein 12), as schematically illustrated in Fig. 4 A. In this approach, a mutant version of 5-ptase with a defective membrane targeting domain (CAAX box) is fused to FKB12 and tagged with monomeric red fluorescent protein (mRFP), whereas its binding partner FRB (fused to CFP) is tethered to the plasma membrane through palmitoylation (construct PM-FRB-CFP; Varnai et al., 2006). In the absence of rapamycin, 5-ptase resides in the cytosol and leaves PtdIns(4,5)P₂ levels at the plasma membrane unaltered (Fig. 4 A, left). Upon addition of 100 nM rapamycin, FKB12 and FRB undergo heterodimerization and the 5-ptase is recruited to the plasma membrane (Fig. 4 A, right).

We expressed the mRFP–FKB12–5-ptase and PM-FRB-CFP fusion proteins in Rat-1 cells and confirmed their proper intracellular localization by confocal microscopy (unpublished data). Addition of rapamycin caused a rapid and complete depletion of PtdIns(4,5)P₂, as shown by the disappearance of the PtdIns(4,5)P₂ sensor YFP-PH from the plasma membrane (Fig. 4, B and C, top trace; $n = 10$). As expected, no Ca²⁺ signal was detected after the 5-ptase–mediated conversion of PtdIns(4,5)P₂ into PtdIns(4)P (Fig. 4 C; $n = 4$). To determine how the 5-ptase–induced hydrolysis of PtdIns(4,5)P₂ affects gap junctional communication, we measured the intercellular diffusion of calcein (added as membrane-permeable calcein-AM) using FRAP (Ponsioen et al., 2007; Fig. 4 D). Rat-1 cells expressing mRFP–FKB12–5-ptase and PM-FRB-CFP showed efficient intercellular transfer of calcein. At 2 min after rapamycin addition, however, intercellular dye diffusion was inhibited as inferred from a strongly reduced fluorescence recovery rate (Fig. 4 D; $n = 15$; $P < 0.005$; ∼0.25× the recovery rate before rapamycin addition). The recovery of calcein fluorescence could not be decreased any further by addition of 50 μM of the gap junction blocker 2-aminoethoxy-diphenylborane (Ponsioen et al., 2007; Fig. 4 D). Rapamycin did not affect cell–cell communication in nontransfected cells (unpublished data). Thus, PtdIns(4,5)P₂ depletion by 5-phosphatase activation is sufficient to inhibit Cx43 gap junctional communication, with no need for PtdIns(4,5)P₂-derived second messengers.
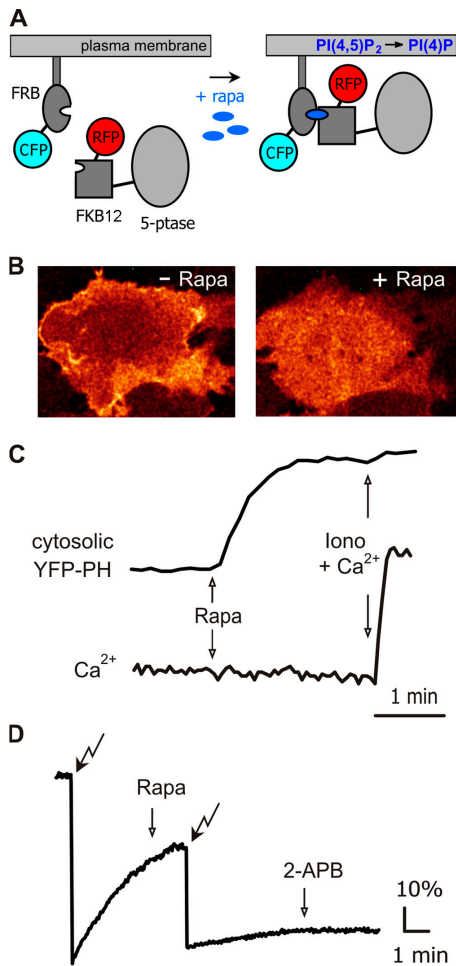
Figure 4. PtdIns(4,5)P₂ depletion by 5-phosphatase inhibits gap junctional communication. (A) Schematic representation of rapamycin-induced PtdIns(4,5)P₂ degradation at the plasma membrane. Rapamycin induces dimerization of FKB12 domains to FRB domains. Rapamycin recruits the phosphoinositide-5-phosphatase-FKB12 fusion protein (mRFP–FKB12–5-ptase) to FRB tethered to the plasma membrane (PM-FRB-CFP), resulting in the rapid conversion of PtdIns(4,5)P₂ into PtdIns(4)P. (B) Confocal images of YFP-PH in Rat-1 cells before (left) and after (right) addition of 100 nM rapamycin. In addition to YFP-PH, PM-FRB-CFP and mRFP–FKB12–5-ptase were also correctly expressed (not depicted). Note that the translocation of YFP-PH into the cytoplasm is complete, indicative of massive PtdIns(4,5)P₂ hydrolysis. (C) Representative responses to rapamycin and ionomycin. (top) Cytosolic levels of YFP-PH; (bottom) Ca²⁺ dye Oregon green. Ionomycin treatment could not induce further translocation of YFP-PH, indicating that rapamycin-induced PtdIns(4,5)P₂ degradation was complete ($n = 10$). Rises in cytosolic Ca²⁺ were never observed ($n = 4$), confirming that PtdIns(4,5)P₂ hydrolysis did not generate second messengers. (D) Gap junctional communication in Rat-1 cells transfected with PM-FRB-CFP and mRFP–FKB12–5-ptase, assayed by FRAP of calcein. Although cells showed efficient communication before rapamycin treatment, gap junctional exchange was significantly decreased at 2 min after addition of rapamycin ($0.25\times$ recovery rate before rapamycin; $n = 15$; $P < 0.005$). The gap junction blocker 2-aminoethoxy-diphenylborane (2-APB) was added at 50 μM.

## Overexpression of PtdIns(4)P 5-kinase (PIP5K) prevents inhibition of cell–cell communication

PtdIns(4,5)P₂ at the plasma membrane is generated mainly from PtdIns(4)P by PIP5K (Hinchliffe et al., 1998; Anderson et al., 1999). As a further test of the PtdIns(4,5)P₂ hypothesis, we stably overexpressed PIP5K (type Iα, fused to GFP) in Rat-1 cells

in an attempt to prevent PtdIns(4,5)P₂ depletion after GPCR stimulation (Fig. 5 A). As shown in Fig. 5 B, transfected GFP-PIP5K localizes to the plasma membrane. In the PIP5K-overexpressing cells, PtdIns(4,5)P₂ levels remain elevated (i.e., above FRET threshold levels) after agonist addition (Fig. 5 C). Nonetheless, GPCR agonists still induced transient rises in IP₃ and Ca²⁺ (Fig. 5 C), indicating that excessive synthesis of PtdIns(4,5)P₂ does not interfere with its hydrolysis. Basal cell–cell communication in PIP5K-overexpressing cells was not significantly different from that in control cells. However, the PIP5K-overexpressing cells failed to close their gap junction channels upon addition of TRP and, to a lesser extent, endothelin (Fig. 5 C). That endothelin is still capable of evoking a residual response in PIP5K-overexpressing cells may be explained by the fact that endothelin is by far the strongest inducer of PtdIns(4,5)P₂ depletion (Fig. 2 D). Expression of a kinase-dead version of PIP5K had no effect on either PtdIns(4,5)P₂ hydrolysis or inhibition of cell–cell communication (Fig. 5 D). We conclude that Cx43 channel closure is prevented when PtdIns(4,5)P₂ is maintained at adequate levels.

No detectable PtdIns(4,5)P₂ binding to the C-terminal tail of Cx43

PtdIns(4,5)P₂ can modulate the activity of various ion channels and transporters, apparently through direct electrostatic interactions (Hilgemann et al., 2001; Suh and Hille, 2005). By analogy, regulation of Cx43 channels by PtdIns(4,5)P₂ would imply that basic residues in Cx43 bind directly to the negatively charged PtdIns(4,5)P₂. Indeed, the regulatory cytosolic tail of Cx43 (aa 228–382) contains a membrane-proximal stretch of both basic and hydrophobic residues ([231]VFFKGVKDRVKGK/R[243]) that could constitute a potential PtdIns(4,5)P₂ binding site. Local depletion of PtdIns(4,5)P₂ might then dissociate the juxtamembrane region of the Cx43 tail from the plasma membrane, leading to channel closure. We reasoned that if the Cx43 juxtamembrane domain binds PtdIns(4,5)P₂ in situ, mutations within this domain might interfere with PtdIns(4,5)P₂-regulated channel closure. We therefore neutralized the membrane-proximal Arg and Lys residues by mutation to alanine, resulting in eight distinct Cx43 mutants, notably, K237A,K241A; R239A,R243A; K241A,R243A; R239A,K241A; K237A,R239A; R239A,K241A,R243A; K237A,R239A,K241A; and the "4A" mutant, K237A,R239A,K241A,K243A. When expressed in Cx43-deficient cells, however, all these mutants were trapped intracellularly and failed to localize to the plasma membrane (Fig. S1, available at http://www.jcb.org/cgi/content/full/jcb .200610144/DC1). Although this result reveals a previously unknown role for the membrane-proximal Arg/Lys residues in Cx43 trafficking, it precludes a test of the Cx43–PtdIns(4,5)P₂ interaction hypothesis.

We next examined whether PtdIns(4,5)P₂ can specifically bind to either the Cx43 C-terminal tail (Cx43CT; aa 228–382) or a Cx43CT-derived juxtamembrane peptide (Cx43JM; aa 228–263) in vitro. We generated a GST-Cx43CT fusion protein and determined its ability to bind phosphoinositides in vitro using three distinct protocols. GST-PH(PLCδ1) was used as a positive control. In the first approach, agarose beads coated with
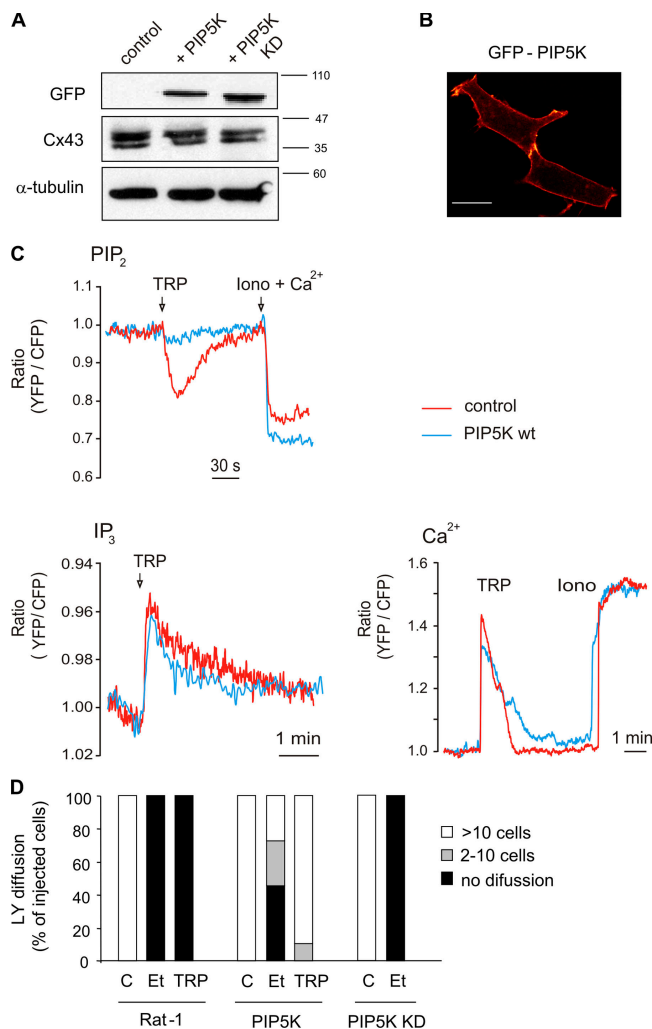
Figure 5. **Overexpression of PIP5K attenuates agonist-induced PtdIns(4,5)P₂ depletion and keeps junctional communication largely intact.** (A) Stable expression of GFP-PIP5K in Rat-1 cells. Total cell lysates were immunoblotted for GFP, Cx43, and α-tubulin as indicated. KD, kinase dead. (B) Localization of GFP-PIP5K in Rat-1 cells. Bar, 10 μm. (C) Temporal changes in the levels of PtdIns(4,5)P₂, IP₃, and Ca²⁺ measured by the respective FRET-based sensors, as detailed in Materials and methods. Control and PIP5K-overexpressing Rat-1 cells were stimulated with 50 μM TRP. In control cells (red trace), PtdIns(4,5)P₂ levels rapidly fall after TRP stimulation, whereas PIP5K overexpression (blue trace) largely prevents the drop in FRET, indicating that PtdIns(4,5)P₂ levels remain high (i.e., above FRET threshold). Ionomycin was used at 5 μM. wt, wild type. n = 5. (D) Bar graphs showing the percentage of communicating cells (LY diffusion) in control Rat-1 cells and cells expressing either wild-type or kinase-dead PIP5K. Cells were left untreated (C) or stimulated with GPCR agonists (50 nM endothelin or 50 μM TRP) as indicated (n ≥ 20 for each dataset). Residual response to endothelin is explained by excessive depletion of PtdIns(4,5)P₂ (compare with Fig. 2 D). LY injections were done at 2 min after addition of agonist.

either PtdIns(4,5)P₂ or PtdIns(4)P were incubated with GST-Cx43CT or GST-PH and then pulled down by centrifugation. PtdIns(4,5)P₂ beads readily brought down the GST-PH polypeptide but not GST-Cx43CT (Fig. S2 A, available at http://www.jcb.org/cgi/content/full/jcb.200610144/DC1). Second, we incubated GST-Cx43CT with ³²P-labeled PtdIns(4,5)P₂ and examined the ability of excess phosphoinositides to displace bound ³²P-PtdIns(4,5)P₂. Although GST-PH showed again

strong PtdIns(4,5)P₂ binding that could readily be displaced by excess PtdIns(4,5)P₂, there was no detectable binding of PtdIns(4,5)P₂ to Cx43CT above that observed with GST alone (Fig. S2 B). Finally, we found that PtdIns(4,5)P₂ (and other phosphoinositides) immobilized on nitrocellulose strips failed to bind either Cx43CT or a 35-amino-acid juxtamembrane domain peptide (Cx43JM; aa 228–263; Giepmans et al., 2001b; unpublished data). Thus, PtdIns(4,5)P₂ does not detectably bind to the juxtamembrane domain of Cx43, or to the full-length regulatory tail (aa 228–362), at least in vitro.

ZO-1 is required for GPCRs to inhibit junctional communication

The very C terminus of Cx43 binds directly to the second PDZ domain of ZO-1, but the functional significance of the Cx43–ZO-1 interaction is not understood. We asked if ZO-1 has a role in modulating gap junctional communication in response to GPCR stimulation. We already showed that RNAi-mediated depletion of Cx43 does not significantly affect the levels and localization of ZO-1 (Fig. 1 B). Conversely, when ZO-1 expression was knocked down by shRNA, Cx43 levels were unaltered (Fig. 6 A). ZO-1–knockdown Rat-1 cells retained their fibroblastic morphology and showed normal Cx43 punctate staining and cell–cell coupling (Fig. 6, B and C), showing that ZO-1 is dispensable for the formation of functional gap junctions. When ZO-1–knockdown cells were stimulated with endothelin, however, the inhibition of cell–cell communication was severely impaired (Fig. 6 C). Importantly, overall PtdIns(4,5)P₂-dependent Ca²⁺ mobilization was not affected in the ZO-1–knockdown cells (Fig. 6 D). We conclude that ZO-1 is essential for the regulation of gap junctional communication by Gq/PLC-coupled receptors, but not for linking those receptors to PLC activation. A plausible explanation for these findings is that ZO-1 serves to bring the PtdIns(4,5)P₂-metabolizing machinery into proximity of Cx43 gap junctions.

Direct interaction between ZO-1 and PLCβ3

As a test of the above hypothesis, we examined whether ZO-1 can interact with PLCβ3. PLCβ3 can associate with at least two scaffold proteins, NHERF2 (in epithelial cells) and Shank2 (in brain), via a C-terminal PDZ domain binding motif (Hwang et al., 2000; Suh et al., 2001). We coexpressed HA-PLCβ3 and GFP–ZO-1 in HEK293 cells and performed immunoprecipitations using anti-GFP antibody (Fig. 7 A). Cell lysates and immunoprecipitates were blotted for GFP and HA. As shown in Fig. 7 B, PLCβ3 and ZO-1 can indeed be coprecipitated. Next, we coexpressed ZO-1 and a PLCβ3 truncation mutant that lacks the C-terminal 14 residues (HA-PLCβ3-ΔPBD; Fig. 7 A) and performed anti-GFP immunoprecipitations. Fig. 7 B shows that truncated PLCβ3 fails to interact with ZO-1, indicating that PLCβ3 interacts with ZO-1 through its very C terminus, containing the PDZ domain binding motif. Considering that ZO-1 has three distinct PDZ domains, we examined which, if any, PDZ domain binds PLCβ3. We expressed GFP-tagged versions of the three individual PDZ domains in HEK293 cells, either alone or together with HA-PLCβ3. We immunoprecipitated PLCβ3 using anti-HA antibody and blotted total cell lysates
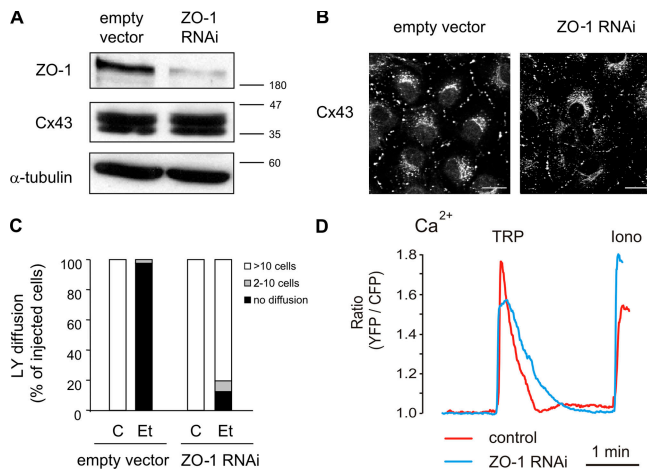
Figure 6. Knockdown of ZO-1 largely prevents agonist-induced disruption of junctional communication while leaving Ca²⁺ mobilization intact. (A) Immunoblots showing strongly reduced ZO-1 expression by adenoviral ZO-1 RNAi compared with control virus (empty vector). ZO-1 knockdown did not affect Cx43 expression, as indicated. (B) Immunostaining of Cx43 in control and ZO-1–knockdown Rat-1 cells. Note that ZO-1 knockdown does not affect Cx43 punctate staining patterns. (C) Bar graphs showing communication in control and ZO-1–knockdown cells (ZO-1 RNAi) before and after addition of 50 nM endothelin (Et; datasets represent totals of at least two independent experiments; number of injected cells: empty vector −/+ Et, n = 53/85; ZO-1 RNAi −/+ Et, n = 43/56). LY injections were done at 2 min after addition of agonist. (D) GPCR-mediated Ca²⁺ mobilization in control cells (red trace) and ZO-1–knockdown cells (blue trace). Ca²⁺ was measured using the FRET-based yellow cameleon probe. TRP was used at 50 µM and Ionomycin at 5 µM. n = 9.

and precipitates for both HA and GFP. As shown in Fig. 7 C, we find that PLCβ3 binds to PDZ3 but not to PDZ1 or PDZ2.

To verify that the ZO-1–PLCβ3 interaction exists endogenously, we precipitated ZO-1 from Rat-1 cells and blotted for both ZO-1 and PLCβ3. Fig. 7 D shows that PLCβ3 coprecipitates with ZO-1. The reverse coprecipitation could not be done, as precipitating antibodies against PLCβ3 are presently not available. Nonetheless, these results suggest that ZO-1, through its respective PDZ2 and PDZ3 domains, assembles Cx43 and PLCβ3 into a signaling complex and thereby facilitates regulation of gap junctional communication by PLC-coupled receptors.

Discussion

A critical and long-standing question in gap junction biology is how junctional communication is regulated by physiological and pathophysiological stimuli. Relatively little progress has been made in identifying receptor-induced signaling events that modulate the channel function of Cx43, the best-studied and most abundant mammalian connexin. In particular, regulation of Cx43 channel activity via G protein signaling has not been systematically examined to date. In the present study, we identify the G_q-linked PLCβ–PtdIns(4,5)P₂ hydrolysis pathway as a key regulator of Cx43-based gap junctional communication in normal fibroblasts. We demonstrate that loss of PtdIns(4,5)P₂ from the plasma membrane is necessary and sufficient to close Cx43 channels, without a role for PtdIns(4,5)P₂-derived second messengers. In other words, PtdIns(4,5)P₂ itself is the responsible signaling molecule. A second novel finding is that the
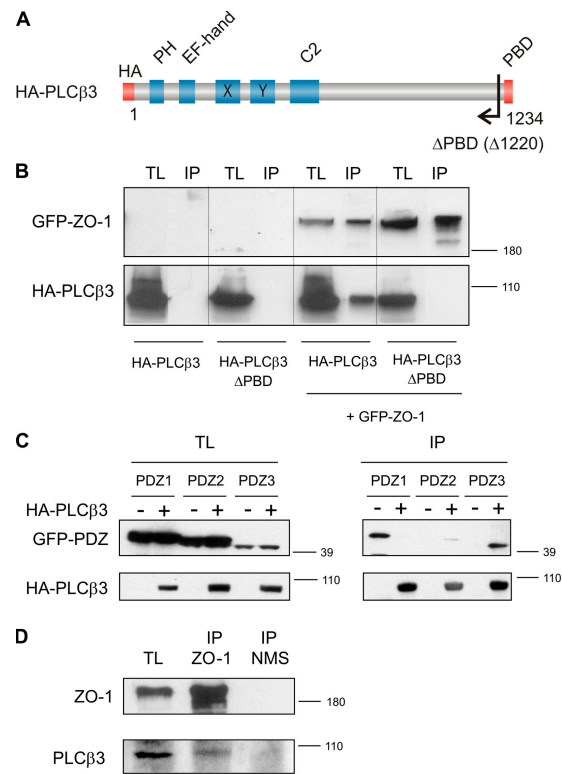
Figure 7. Association of ZO-1 with PLCβ3. (A) Schematic representation of HA-PLCβ3. X and Y represent the catalytic domains; the C2 domain interacts with activated $G\alpha_q$ (Rhee, 2001). ΔPBD indicates mutant PLCβ3 lacking the C-terminal residues 1220–1234 (comprising the PDZ domain binding motif). (B) Coimmunoprecipitation of GFP–ZO-1 and HA-PLCβ3 expressed in HEK293 cells. Samples were immunoblotted for GFP (top) and HA (bottom). IP denotes immunoprecipitation using anti-GFP antiserum. TL, total cell lysates. (C) Coimmunoprecipitation of HA-PLCβ3 and GFP-tagged individual PDZ domains of ZO-1 expressed in HEK293 cells. Samples were immunoblotted for GFP (top) and HA (bottom). IP denotes immunoprecipitation using anti-HA antibody. (D) Endogenous ZO-1 immunoprecipitated from Rat-1 cells. Total cell lysates and samples from ZO-1 immunoprecipitates were blotted for both ZO-1 and PLCβ3 as indicated. NMS, normal mouse serum.

Cx43 binding partner ZO-1 binds to PLCβ3 and is essential for PtdIns(4,5)P₂-hydrolyzing receptors to regulate gap junctional communication.

PtdIns(4,5)P₂ as a key regulator
Our conclusion that PtdIns(4,5)P₂ at the plasma membrane regulates Cx43 channel function is based on several lines of evidence. First, active $G\alpha_q$ (but not $G\alpha_i$, $G\alpha_{12}$, or $G\alpha_{13}$) depletes PtdIns(4,5)P₂ from the plasma membrane and abrogates gap junctional communication. Second, knockdown of PLCβ3 inhibits agonist-induced PtdIns(4,5)P₂ depletion and prevents disruption of cell–cell communication. Third, conversion of PtdIns(4,5)P₂ into PtdIns(4)P by a translocatable 5-phosphatase is sufficient to inhibit intercellular communication. Fourth, maintaining PtdIns(4,5)P₂ at adequate levels by overexpression of PIP5K renders Cx43 channels refractory to GPCR stimulation, although second messenger generation still occurs.

Acting as a signaling molecule in its own right, PtdIns(4,5)P₂ can regulate local cellular activities when its levels rise and fall; in particular, PtdIns(4,5)P₂ can modulate the activity of

various ion channels and transporters, presumably through electrostatic interactions (Hilgemann et al., 2001; Suh and Hille, 2005). Although the existence of such interactions in living cells remains largely inferential and PtdIns(4,5)P_2 binding consensus sequences have not been clearly defined, the common theme is that the negatively charged PtdIns(4,5)P_2 binds to a motif with multiple positive charges interdispersed with hydrophobic residues (Janmey et al., 1992; McLaughlin and Murray, 2005). The Cx43 C-terminal juxtamembrane domain indeed contains such a putative PtdIns(4,5)P_2 binding motif (aa 231–243), although this stretch also meets the criteria of a tubulin binding domain (Giepmans et al., 2001b). Extension of the above model to Cx43 channel gating would then imply that local loss of PtdIns(4,5)P_2 could release the Cx43 regulatory tail from the plasma membrane to render it susceptible to a modification, leading to channel closure. However, our investigations to detect specific binding of PtdIns(4,5)P_2 to the Cx43 C-terminal tail or its juxtamembrane domain in vitro yielded negative results. Rather, mutational analysis revealed that those basic residues in the juxtamembrane domain have a hitherto unrecognized role in the trafficking of Cx43 to the plasma membrane. These findings do not, of course, rule out the possibility that PtdIns(4,5)P_2 does bind directly to Cx43 in situ.

Aside from modulating ion channel activity, PtdIns(4,5)P_2 has been implicated in cytoskeletal remodeling, vesicular trafficking, and recruitment of cytosolic proteins to specific membranes (Yin and Janmey, 2003; McLaughlin and Murray, 2005). Although Cx43 can interact with cytoskeletal proteins, such as tubulin and drebrin (Giepmans et al., 2001b; Butkevich et al., 2004), cytoskeletal reorganization does not play a significant role in regulating Cx43 junctional communication because cytoskeleton-disrupting agents (cytochalasin D, nocodazole, and Rho-inactivating C3 toxin) have no detectable effect on GPCR regulation of cell–cell coupling (Giepmans et al., 2001b; Table S1). Furthermore, we found that GPCR-induced inhibition and recovery of gap junctional communication are insensitive to agents known to interfere with Cx43 trafficking and internalization, including cycloheximide, brefeldin A, monensin, ammonium chloride, and hypertonic sucrose (Table S1).

Numerous studies have suggested that closure of Cx43 channels in response to divergent stimuli somehow results from Cx43 phosphorylation (Lampe and Lau, 2004; Laird, 2005). Several protein kinases, including PKC, MAP kinase, casein kinase-1, and Src, are capable of phosphorylating Cx43 at multiple sites in the C-terminal tail. These phosphorylations have been implicated not only in Cx43 channel gating but also in Cx43 trafficking, assembly, and degradation. The link between Cx43 phosphorylation and altered cell–cell coupling is largely correlative, however, as the functional significance of most of these phosphorylations has not been elucidated. Our previous studies suggested that c-Src–mediated tyrosine phosphorylation of Cx43 underlies disruption of gap junctional communication, as inferred from experiments using both constitutively active and dominant-negative versions of c-Src (Postma et al., 1998; Giepmans et al., 2001a). To date, however, we have been unable to detect GPCR-induced tyrosine phosphorylation of Cx43 in a
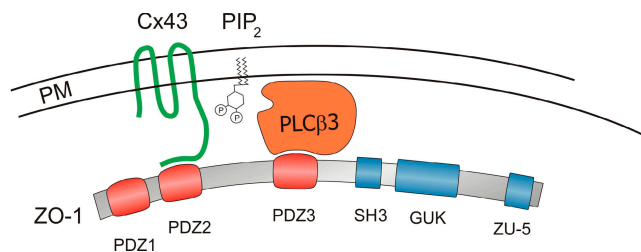
Figure 8. **Schematic drawing of the proposed model.** ZO-1 is proposed to assemble Cx43 and PLCβ3 into a complex, thereby facilitating regulation of Cx43 channel function by localized changes in PtdIns(4,5)P_2 upon receptor activation. As we found no evidence for direct binding of PtdIns(4,5)P_2 to Cx43, PtdIns(4,5)P_2 might regulate junctional communication in an indirect manner, for example, via a Cx43-associated protein that modifies the Cx43 regulatory tail and thereby shuts off channel function. PM, plasma membrane.

physiological context. Furthermore, the Src inhibitor PP2 does not prevent GPCR agonists from inhibiting Cx43-based gap junctional communication in either Rat-1 cells or primary astrocytes (Table S1; Rouach et al., 2006). Therefore, tyrosine phosphorylation of Cx43 leading to loss of cell–cell coupling, as observed with constitutively active c-Src and v-Src (Warn-Cramer and Lau, 2004), may not actually occur under physiological conditions, an issue that warrants further investigation.

Essential role for ZO-1

Another novel finding of the present study concerns the role of ZO-1, an established binding partner of Cx43 (Giepmans and Moolenaar, 1998; Toyofuku et al., 1998). Originally identified as a major component of epithelial tight junctions (Stevenson et al., 1986), ZO-1 is thought to serve as a platform to scaffold various transmembrane and cytoplasmic proteins. ZO-1 and its close relative ZO-2 have several protein-interaction domains, including three PDZ domains, one SH3 domain, and one GUK domain. In epithelial cells, ZO-1 and -2 act redundantly to some extent in the formation of tight junctions (Umeda et al., 2004; Rouach et al., 2006). In nonepithelial cells lacking tight junctions, ZO-1 has been attributed a role in the assembly and stabilization of Cx43 gap junctions (Hunter et al., 2005; Singh et al., 2005), but its precise role has remained elusive. Our knockdown studies herein show that ZO-1 is essential for G_q/PLC-coupled receptors to inhibit intercellular communication, but not for coupling those receptors to PLC activation, as inferred from Ca^{2+} mobilization experiments; this result suggests that loss of ZO-1 at Cx43 gap junctions is not compensated for by ZO-2. We find that ZO-1 binds directly to the very C terminus of PLCβ3 via its third PDZ domain. In the simplest model compatible with our findings, ZO-1 serves to assemble Cx43 and PLCβ3 into a complex to permit regulation of gap junctional communication by localized changes in PtdIns(4,5)P_2, as schematically illustrated in Fig. 8. As we found no evidence for direct binding of PtdIns(4,5)P_2 to Cx43 in vitro, PtdIns(4,5)P_2 might regulate junctional communication in an indirect manner, for example, via a Cx43-associated protein that modifies the Cx43 regulatory tail and thereby shuts off channel function. Precisely how PtdIns(4,5)P_2 regulates the Cx43 multiprotein complex remains a challenge for future studies.

Materials and methods

Reagents
Materials were obtained from the following sources: endothelin, TRP (sequence SFLLRN), neurokinin A, Cx43 polyclonal, and α-tubulin monoclonal antibodies from Sigma-Aldrich; *P. multocida* toxin from Calbiochem-Novabiochem; Cx43 NT monoclonal antibody from the Fred Hutchinson Cancer Research Center; actin monoclonal from Chemicon International; polyclonal PLCβ3 antibody from Cell Signaling; ZO-1 monoclonal antibody from Zymed Laboratories; HRP-conjugated secondary antibodies from DakoCytomation, and secondary antibodies for immunofluorescence (goat anti–mouse [Alexa488] and goat anti–rabbit [Alexa594]) from Invitrogen. HA, Myc, and GST monoclonal antibodies were purified from hybridoma cell lines 12CA5, 9E10, and 2F3, respectively. GFP antiserum was generated in our institute.

cDNA constructs
Constructs encoding active (GTPase-deficient) Gα subunits, EGFP-PH$_{PLCδ1}$, ECFP-PH$_{PLCδ1}$, EYFP-PH$_{PLCδ1}$, and EGFP-tagged mouse type Iα PIP5K have been described (Kranenburg et al., 1999; van der Wal et al., 2001; van Horck et al., 2002). Mouse PLCβ3 cDNA was obtained from MRC Geneservice, cloned into pcDNA3-HA by PCR (see Table S2, available at http://www.jcb.org/cgi/content/full/jcb.200610144/DC1, for primers) and ligated into pcDNA3-HA XhoI–NotI sites. HA-PLCβ3-ΔPBD was obtained by restriction of the full-length construct with Eco47III, cleaving off the very C-terminal 14 residues. Human ZO-1 was cloned into XhoI and KpnI sites of pEGFP C2 (CLONTECH Laboratories, Inc.). GFP-based yellow cameleon 2.1 has been described (van der Wal et al., 2001). Constructs encoding cytosolic 5-phosphatase fused to FKB12-mRFP and PM-FRB-CFP have been described (Varnai et al., 2006).

Cell culture and cell–cell communication assays
Cells were cultured in DME containing 8% fetal calf serum, L-glutamine, and antibiotics. For cell–cell communication assays, cells were grown in 3-cm dishes and serum starved for at least 4 h before experimentation. Monitoring the diffusion of LY from single microinjected cells and single-electrode electrophysiological measurements of cell–cell coupling were done as described previously (Postma et al., 1998). Images were acquired on an inverted microscope (Axiovert 135; Carl Zeiss MicroImaging, Inc.), equipped with an Achroplan 40× objective (NA 0.60) and a camera (F301; Nikon).

SDS-PAGE, immunoblotting, and immunoprecipitation
Cells were harvested in Laemmli sample buffer (LSB), boiled for 10 min, and subjected to immunoblot analysis according to standard procedures. Filters were blocked in TBST/5% milk, incubated with primary and secondary antibodies, and visualized by enhanced chemoluminescence (GE Healthcare). For immunoprecipitation, cells were harvested in 1% NP-40 and 0.25% sodium desoxycholate lysis buffer. Lysates were spun down, and the supernatants were subjected to immunoprecipitation using protein A–conjugated antibodies for 4 h at 4°C. Proteins were eluted by boiling for 10 min in LSB and analyzed by immunoblotting.

Immunostaining and fluorescence microscopy
Cells grown on coverslips were fixed in 3.7% formaldehyde in PBS for 15 min. Samples were blocked and permeabilized in PBS containing 1% BSA and 0.1% Triton X-100 for 30 min. Subsequently, samples were incubated with primary and secondary antibodies for 30 min each in PBS/1% BSA, washed five times with PBS, and mounted in MOWIOL (Calbiochem). Confocal fluorescence images were obtained on a confocal system (TCS NT; Leica), equipped with an Ar/Kr laser. Images were taken using a 63× NA 1.32 oil objective. Standard filter combinations and Kalman averaging were used. Processing of images for presentation was done on a PC using Photoshop (Adobe).

Live-cell imaging
All live imaging and time-lapse experiments were performed in bicarbonate-buffered saline containing 140 mM NaCl, 5 mM KCl, 1 mM MgCl$_2$, 1 mM CaCl$_2$, 10 mM glucose, 23 mM NaHCO$_3$, and 10 mM Hepes, pH 7.2, kept under 5% CO$_2$, at 37°C. Images of live cells expressing GFP-PH and GFP-PIP5K were recorded on a confocal microscope (TCS-SP2; Leica) using a 63× lens (NA 1.4).

PtdIns(4,5)P$_2$, IP$_3$, and Ca^{2+} imaging by FRET ratiometry
Temporal changes in PtdIns(4,5)P$_2$ levels in living cells were assayed by the FRET-based PtdIns(4,5)P$_2$ sensor, PH-PLCδ1, as described previously (van der Wal et al., 2001). In brief, Rat-1 cells were transiently transfected with CFP-PH and YFP-PH constructs (1:1 ratio) using Fugene transfection agent and placed on a inverted microscope (Nikon) equipped with an Achroplan 63× oil objective (NA 1.4). Excitation was at 425 ± 5 nm. CFP and YFP emissions were detected simultaneously at 475 ± 15 and 540 ± 20 nm, respectively, and recorded with PicoLog Data Acquisition Software (Pico Technology). FRET is expressed as the ratio of acceptor to donor fluorescence. At the onset of the experiment, the ratio was adjusted to 1.0, and FRET changes were expressed as relative deviations from baseline. Temporal changes in IP$_3$ levels were monitored using a FRET-based IP$_3$ sensor, in which the IP$_3$ binding domain of the human type I IP$_3$ receptor (aa 224–605) is fused between CFP and YFP, essentially analogous to the sensor described previously (Tanimura et al., 2004). In vitro binding studies showed that it bound IP$_3$ with an apparent K_d of ~5 nM. Intracellular Ca^{2+} mobilization was monitored using the CFP/YFP-based Ca^{2+} sensor yellow cameleon 2.1 (Miyawaki et al., 1997; Rhee, 2001; van der Wal et al., 2001). Traces were smoothened in Excel (Microsoft) using a moving average function ranging from 3 to 6.

PtdIns(4,5)P$_2$ depletion by rapamycin-induced translocation of phosphoinositide 5-phosphatase
Rat-1 cells were transiently transfected with PM-CFP-FRB and mRFP–FKB12–5-ptase (Varnai et al., 2006). Cells were selected for experimentation when sufficient protein levels were expressed as judged by CFP and mRFP fluorescence. For PtdIns(4,5)P$_2$ measurements, the YFP-PH construct was cotransfected. For Ca^{2+} measurements, cells were loaded with Oregon green-AM. To monitor gap junctional communication, cells were loaded with calcein-AM and analyzed by FRAP (Ponsioen et al., 2007). These experiments were performed on a confocal microscope (TCS-SP2; Leica) using 63× lens (NA 1.4).

Overexpression of PIP5K
To overexpress PIP5K (type Iα; van Horck et al., 2002), virus containing the LZRS-PIP5K constructs was generated as described in the following paragraph. Rat-1 cells were incubated with 1 ml viral supernatant supplemented with 10 μl Dotap (Roche). 48 h after infection, cells were plated in selection medium. Transfected cells were selected on 200 μg/ml zeocin (Invitrogen) for 2 wk, and colonies were examined for PIP5K expression.

RNAi
To generate Cx43-deficient Rat-1 cells, Cx43 was knocked down by stable expression of retroviral pSuper (pRS; Brummelkamp et al., 2002) containing the RNAi target sequence GGTGTGGCTGTCAGTGCTC. pRS-Cx43 was transfected into Phoenix-Eco package cells, and the supernatant containing viral particles was harvested after 72 h. For infection, cells were incubated with 1 ml viral supernatant supplemented with 10 μl Dotap (1 mg/ml). 48 h after infection, cells were selected on 2 μg/ml puromycin for 2 wk. Single cell-derived colonies were tested for Cx43 expression and communication. PLCβ3 was stably knocked down by retroviral expression of PLCβ3 shRNA. Four different target sequences were selected, namely, ACTACGTCTGCCTGCGAAATT, GATTCGAGAGGTACTGGGC, TTACGTTGAGCCCGTCAAG, and CCCTTTGACTTCCCCAAGG). Nonfunctional shRNA was used as a control. ZO-1 was transiently knocked down by adenoviral expression of ZO-1 RNAi. First, ZO-1 RNAi oligos containing the ZO-1 target sequence GGAGGGCCAGCTGAAGGAC were ligated into pSuper after oligo annealing. Next, the oligos, together with the H1 RNA promotor, were subcloned into pEntr1A (BamHI–XhoI) and recombinated into pAd/PL-Dest according to protocol (Virapower Adenoviral Expression System; Invitrogen). Virus was produced in 293A packaging cells according to standard procedures. Supernatant containing virus particles was titrated on Rat-1 cells to determine the amount needed for ZO-1 knockdown.

Online supplemental material
Fig. S1 shows intracellular accumulation of the Cx43-4A mutant. Fig. S2 shows lack of detectable binding of phosphoinositides to the Cx43 C-terminal tail. Table S1 summarizes the results of pharmacological experiments. Table S2 shows sequences of the oligos used. Online supplemental material is available at www.jcb.org/cgi/content/full/jcb.200610144/DC1.

References

Alblas, J., I. van Etten, and W.H. Moolenaar. 1996. Truncated, desensitization-defective neurokinin receptors mediate sustained MAP kinase activation, cell growth and transformation by a Ras-independent mechanism. *EMBO J.* 15:3351–3360.

Anderson, R., I. Boronenkov, S. Doughman, J. Kunz, and J. Loijens. 1999. Phosphatidylinositol phosphate kinases, a multifaceted family of signaling enzymes. *J. Biol. Chem.* 274:9907–9910.

Bernstein, S.A., and G.E. Morley. 2006. Gap junctions and propagation of the cardiac action potential. *Adv. Cardiol.* 42:71–85.

Blomstrand, F., L. Venance, A.L. Siren, P. Ezan, E. Hanse, J. Glowinski, H. Ehrenreich, and C. Giaume. 2004. Endothelins regulate astrocyte gap junctions in rat hippocampal slices. *Eur. J. Neurosci.* 19:1005–1015.

Bremnes, T., J.D. Paasche, A. Mehlum, C. Sandberg, B. Bremnes, and H. Attramadal. 2000. Regulation and intracellular trafficking pathways of the endothelin receptors. *J. Biol. Chem.* 275:17596–17604.

Brummelkamp, T., R. Bernards, and R. Agami. 2002. A system for stable expression of short interfering RNAs in mammalian cells. *Science.* 296:550–553.

Butkevich, E., S. Hulsmann, D. Wenzel, T. Shirao, R. Duden, and I. Majoul. 2004. Drebrin is a novel connexin-43 binding partner that links gap junctions to the submembrane cytoskeleton. *Curr. Biol.* 14:650–658.

Cramer, H., W. Muller-Esterl, and C. Schroeder. 1997. Subtype-specific desensitization of human endothelin ETA and ETB receptors reflects differential receptor phosphorylation. *Biochemistry.* 36:13325–13332.

Gerido, D.A., and T.W. White. 2004. Connexin disorders of the ear, skin, and lens. *Biochim. Biophys. Acta.* 1662:159–170.

Giepmans, B. 2004. Gap junctions and connexin-interacting proteins. *Cardiovasc. Res.* 62:233–245.

Giepmans, B., and W.H. Moolenaar. 1998. The gap junction protein connexin43 interacts with the second PDZ domain of the zona occludens-1 protein. *Curr. Biol.* 8:931–934.

Giepmans, B., T. Hengeveld, F. Postma, and W.H. Moolenaar. 2001a. Interaction of c-Src with gap junction protein connexin-43. Role in the regulation of cell-cell communication. *J. Biol. Chem.* 276:8544–8549.

Giepmans, B., I. Verlaan, T. Hengeveld, H. Janssen, J. Calafat, M. Falk, and W.H. Moolenaar. 2001b. Gap junction protein connexin-43 interacts directly with microtubules. *Curr. Biol.* 11:1364–1368.

Goodenough, D.A., J.A. Goliger, and D.L. Paul. 1996. Connexins, connexons, and intercellular communication. *Annu. Rev. Biochem.* 65:475–502.

Halstead, J.R., J. van Rheenen, M.H. Snel, S. Meeuws, S. Mohammed, C.S. D'Santos, A.J. Heck, K. Jalink, and N. Divecha. 2006. A role for PtdIns(4,5)P2 and PIP5Kalpha in regulating stress-induced apoptosis. *Curr. Biol.* 16:1850–1856.

Harris, A.L. 2001. Emerging issues of connexin channels: biophysics fills the gap. *Q. Rev. Biophys.* 34:325–472.

Hilgemann, D.W., S. Feng, and C. Nasuhoglu. 2001. The complex and intriguing lives of PIP2 with ion channels and transporters. *Sci. STKE.* 2001:RE19.

Hill, C.S., S.Y. Oh, S.A. Schmidt, K.J. Clark, and A.W. Murray. 1994. Lysophosphatidic acid inhibits gap-junctional communication and stimulates phosphorylation of connexin-43 in WB cells: possible involvement of the mitogen-activated protein kinase cascade. *Biochem. J.* 303:475–479.

Hinchliffe, K.A., A. Ciruela, and R.F. Irvine. 1998. PI(1-2)Pkins1, their substrates and their products: new functions for old enzymes. *Biochim. Biophys. Acta.* 1436:87–104.

Hunter, A., R. Barker, C. Zhu, and R. Gourdie. 2005. Zonula occludens-1 alters connexin43 gap junction size and organization by influencing channel accretion. *Mol. Biol. Cell.* 16:5686–5698.

Hwang, J., K. Heo, K. Shin, E. Kim, C.-H.C. Yun, S. Ryu, H. Shin, and P. Suh. 2000. Regulation of phospholipase C-beta 3 activity by Na+/H+ exchanger regulatory factor 2. *J. Biol. Chem.* 275:16632–16637.

Janmey, P.A., J. Lamb, P.G. Allen, and P.T. Matsudaira. 1992. Phosphoinositide-binding peptides derived from the sequences of gelsolin and villin. *J. Biol. Chem.* 267:11818–11823.

Kranenburg, O., M. Poland, F. van Horck, D. Drechsel, A. Hall, and W.H. Moolenaar. 1999. Activation of RhoA by lysophosphatidic acid and Galpha 12/13 subunits in neuronal cells: induction of neurite retraction. *Mol. Biol. Cell.* 10:1851–1857.

Kwak, B.R., M.S. Pepper, D.B. Gros, and P. Meda. 2001. Inhibition of endothelial wound repair by dominant negative connexin inhibitors. *Mol. Biol. Cell.* 12:831–845.

Laing, J., B. Chou, and T. Steinberg. 2005. ZO-1 alters the plasma membrane localization and function of Cx43 in osteoblastic cells. *J. Cell Sci.* 118:2167–2176.

Laird, D. 2005. Connexin phosphorylation as a regulatory event linked to gap junction internalization and degradation. *Biochim. Biophys. Acta.* 1711:172–182.

Lampe, P., and A. Lau. 2004. The effects of connexin phosphorylation on gap junctional communication. *Int. J. Biochem. Cell Biol.* 36:1171–1186.

McLaughlin, S., and D. Murray. 2005. Plasma membrane phosphoinositide organization by protein electrostatics. *Nature.* 438:605–611.

Meme, W., P. Ezan, L. Venance, J. Glowinski, and C. Giaume. 2004. ATP-induced inhibition of gap junctional communication is enhanced by interleukin-1 beta treatment in cultured astrocytes. *Neuroscience.* 126:95–104.

Mesnil, M., S. Crespin, J. Avanzo, and M. Zaidan-Dagli. 2005. Defective gap junctional intercellular communication in the carcinogenic process. *Biochim. Biophys. Acta.* 1719:125–145.

Miyawaki, A., J. Llopis, R. Heim, J.M. McCaffery, J. Adams, M. Ikura, and R. Tsien. 1997. Fluorescent indicators for Ca^{2+} based on green fluorescent proteins and calmodulin. *Nature.* 388:882–887.

Mori, R., K.T. Power, C.M. Wang, P. Martin, and D.L. Becker. 2006. Acute downregulation of connexin43 at wound sites leads to a reduced inflammatory response, enhanced keratinocyte proliferation and wound fibroblast migration. *J. Cell Sci.* 119:5193–5203.

Neijssen, J., C. Herberts, J. Drijfhout, E. Reits, L. Janssen, and J. Neefjes. 2005. Cross-presentation by intercellular peptide transfer through gap junctions. *Nature.* 434:83–88.

Oliveira, R., C. Christov, J.S. Guillamo, S. de Bouard, S. Palfi, L. Venance, M. Tardy, and M. Peschanski. 2005. Contribution of gap junctional communication between tumor cells and astroglia to the invasion of the brain parenchyma by human glioblastomas. *BMC Cell Biol.* 6:7.

Orth, J., S. Lang, M. Taniguchi, and K. Aktories. 2005. *Pasteurella multocida* toxin-induced activation of RhoA is mediated via two families of Gα proteins, Gα_q and G$\alpha_{12/13}$. *J. Biol. Chem.* 280:36701–36707.

Ponsioen, B., L. van Zeijl, W.H. Moolenaar, and K. Jalink. 2007. Direct measurement of cyclic AMP diffusion and signaling through connexin43 gap junctional channels. *Exp. Cell Res.* 313:415–423.

Postma, F., T. Hengeveld, J. Alblas, B. Giepmans, G. Zondag, K. Jalink, and W.H. Moolenaar. 1998. Acute loss of cell-cell communication caused by G protein-coupled receptors: a critical role for c-Src. *J. Cell Biol.* 140:1199–1209.

Qiu, C., P. Coutinho, S. Frank, S. Franke, L.Y. Law, P. Martin, C.R. Green, and D.L. Becker. 2003. Targeting connexin43 expression accelerates the rate of wound repair. *Curr. Biol.* 13:1697–1703.

Reaume, A.G., P. A. de Sousa, S. Kulkarni, B.L. Langille, D. Zhu, T.C. Davies, S.C. Juneja, G.M. Kidder, and J. Rossant. 1995. Cardiac malformation in neonatal mice lacking connexin43. *Science.* 267:1831–1834.

Rhee, S. 2001. Regulation of phosphoinositide-specific phospholipase C. *Annu. Rev. Biochem.* 70:281–312.

Rouach, N., A. Pebay, W. Meme, J. Cordier, P. Ezan, E. Etienne, C. Giaume, and M. Tence. 2006. S1P inhibits gap junctions in astrocytes: involvement of G and Rho GTPase/ROCK. *Eur. J. Neurosci.* 23:1453–1464.

Saez, J.C., V.M. Berthoud, M.C. Branes, A.D. Martinez, and E.C. Beyer. 2003. Plasma membrane channels formed by connexins: their regulation and functions. *Physiol. Rev.* 83:1359–1400.

Singh, D., J.L. Solan, S.M. Taffet, R. Javier, and P.D. Lampe. 2005. Connexin 43 interacts with zona occludens-1 and -2 proteins in a cell cycle stage-specific manner. *J. Biol. Chem.* 280:30416–30421.

Sohl, G., and K. Willecke. 2004. Gap junctions and the connexin protein family. *Cardiovasc. Res.* 62:228–232.

Spinella, F., L. Rosano, V. Di Castro, M. Nicotra, P. Natali, and A. Bagnato. 2003. Endothelin-1 decreases gap junctional intercellular communication by inducing phosphorylation of connexin 43 in human ovarian carcinoma cells. *J. Biol. Chem.* 278:41294–41301.

Stauffer, T., S. Ahn, and T. Meyer. 1998. Receptor-induced transient reduction in plasma membrane PtdIns(4,5)P2 concentration monitored in living cells. *Curr. Biol.* 8:343–346.

Stevenson, B.R., J.D. Siliciano, M.S. Mooseker, and D.A. Goodenough. 1986. Identification of ZO-1: a high molecular weight polypeptide associated with the tight junction (zonula occludens) in a variety of epithelia. *J. Cell Biol.* 103:755–766.

Suh, B.C., and B. Hille. 2005. Regulation of ion channels by phosphatidylinositol 4,5-bisphosphate. *Curr. Opin. Neurobiol.* 15:370–378.

Suh, B.C., T. Inoue, T. Meyer, and B. Hille. 2006. Rapid chemically induced changes of PtdIns(4,5)P2 gate KCNQ ion channels. *Science.* 314:1454–1457.

Suh, P., J. Hwang, S. Ho Ryu, M. Donowitz, and J. Ho Kim. 2001. The roles of PDZ-containing proteins in PLC-β-mediated signaling. *Biochem. Biophys. Res. Commun.* 288:1–7.

Tanimura, A., A. Nezu, T. Morita, R.J. Turner, and Y. Tojyo. 2004. Fluorescent biosensor for quantitative real-time measurements of inositol 1,4,5-trisphosphate in single living cells. *J. Biol. Chem.* 279:38095–38098.

Toyofuku, T., M. Yabuki, K. Otsu, T. Kuzuya, M. Hori, and M. Tada. 1998. Direct association of the gap junction protein connexin-43 with ZO-1 in cardiac myocytes. *J. Biol. Chem.* 273:12725–12731.

Umeda, K., T. Matsui, M. Nakayama, K. Furuse, H. Sasaki, M. Furuse, and S. Tsukita. 2004. Establishment and characterization of cultured epithelial cells lacking expression of ZO-1. *J. Biol. Chem.* 279:44785–44794.

van der Wal, J., R. Habets, P. Varnai, T. Balla, and K. Jalink. 2001. Monitoring agonist-induced phospholipase C activation in live cells by fluorescence resonance energy transfer. *J. Biol. Chem.* 276:15337–15344.

van Dijk, M., F.J. Muriana, P.C. Der Hoeven, J. de Widt, D. Schaap, W.H. Moolenaar, and W.J. van Blitterswijk. 1997. Diacylglycerol generated by exogenous phospholipase C activates the mitogen-activated protein kinase pathway independent of Ras- and phorbol ester-sensitive protein kinase C: dependence on protein kinase C-zeta. *Biochem. J.* 323:693–699.

van Horck, F., E. Lavazais, B. Eickholt, W.H. Moolenaar, and N. Divecha. 2002. Essential role of Type Iα phosphatidylinositol 4-phosphate 5-kinase in neurite remodeling. *Curr. Biol.* 12:241–245.

Varnai, P., and T. Balla. 1998. Visualization of phosphoinositides that bind pleckstrin homology domains: calcium- and agonist-induced dynamic changes and relationship to myo-[3H]inositol-labeled phosphoinositide pools. *J. Cell Biol.* 143:501–510.

Varnai, P., B. Thyagarajan, T. Rohacs, and T. Balla. 2006. Rapidly inducible changes in phosphatidylinositol 4,5-bisphosphate levels influence multiple regulatory functions of the lipid in intact living cells. *J. Cell Biol.* 175:377–382.

Venance, L., D. Piomelli, J. Glowinski, and C. Glaume. 1995. Inhibition by anandamide of gap junctions and intercellular calcium signalling in striatal astrocytes. *Nature.* 376:590–594.

Warn-Cramer, B., and A. Lau. 2004. Regulation of gap junctions by tyrosine protein kinases. *Biochim. Biophys. Acta.* 1662:81–95.

Wei, C., X. Xu, and C. Lo. 2004. Connexins and cell signaling in development and disease. *Annu. Rev. Cell Dev. Biol.* 20:811–838.

Yin, H.L., and P.A. Janmey. 2003. Phosphoinositide regulation of the actin cytoskeleton. *Annu. Rev. Physiol.* 65:761–789.